ISET Journal of Earthquake Technology, Paper No. 599, Vol. 62, No. 2, June 2025, pp. 141-156

INNOVATIVE APPROACHES FOR ADDRESSING CHALLENGES IN HIGH-SPEED RAILWAY GEOTECHNICS

S. Nimbalkar*
Associate Professor, School of Civil and Environmental Engineering
University of Technology Sydney (UTS), Australia;
Visiting Associate Professor, Indian Institute of Technology Bombay (IITB)
Mumbai, Maharashtra 400076, India;
Adjunct Faculty, Indian Institute of Technology Madras (IITM)
Chennai, Tamil Nadu 600036, India, Email id: Sanjay.Nimbalkar@uts.edu.au

P. Punetha
Research Fellow, School of Civil and Environmental Engineering
University of Technology Sydney (UTS), Australia, Email id: Piyush.Punetha@uts.edu.au

M.A. Farooq
Research Associate, School of Civil and Environmental Engineering
University of Technology Sydney (UTS), Australia, Email id: MohammadAdnan.Farooq@uts.edu.au

N.K. Meena
Geotechnical Engineer, Beca Pty. Ltd., Sydney, Australia, Email id: Naveen.Meena@beca.com

H. Farooq
Research Associate, School of Civil and Environmental Engineering
University of Technology Sydney (UTS), Australia, Email id: Hafsa.Farooq@uts.edu.au

ABSTRACT

High-speed rail (HSR) is among the most significant innovations in the transportation sector, and it continues to gain global prominence. However, the development and design of HSR network pose unique challenges. This keynote paper highlights some of these challenges and proposes solutions using innovative materials and computational approaches. First, the effectiveness of a novel composite material designed to alleviate vibrations generated from high-speed train movements is evaluated through laboratory testing. The finite element method (FEM) is then utilized to compare the performance of ballasted and ballastless (or slab) tracks, aiding in the selection of the most appropriate track type for HSR operations. A comprehensive review of existing rheological models for predicting railway track performance is provided, and a novel computational method to analyze the dynamic behavior of standard railway tracks and transition zones under moving loads, accounting for principal stress rotation effects, is introduced. Furthermore, the effect of seismic loading on the lateral stability of tracks and the soil arching mechanism in pile foundation supported railway embankments is explored. The findings from this paper offer valuable insights into overcoming the key engineering challenges in HSR infrastructure design and development.

KEYWORDS: High-Speed Rail, Vibration Mitigation, Finite Element Method, Seismic Loading, Transition Zone, Soil Arching

INTRODUCTION

The need for efficient transportation infrastructure is escalating as population growth accelerates and congestion intensifies in major cities around the world. In response, global investments in the transportation sector have surged, focusing on developing innovative technologies to improve infrastructure, reduce travel times, and enhance passenger safety and comfort. For instance, in 2024, the Australian government announced a $16.5 billion investment in transportation infrastructure as part of its budget (Australian Federal Government, 2024).

High speed rail (HSR) is a prime example of technological advancement in the transport sector, which is quickly gaining global prominence. Often described as the transport mode of the future, HSR features

https://doi.org/10.63898/CXYO2445
*Corresponding Author

fast trains, robust tracks, advanced train management systems and other state-of-the-art infrastructure (UIC, 2018). While there are several definitions of HSR, the International Union of Railways (UIC) primarily defines it as a system that operates at an average speed of 250 km/h or more (UIC, 2018). Key factors driving the popularity of HSR include significant reduction in travel time, affordable fares, and safe operations. The impressive performance of HSR in countries such as China, France, Germany, Italy and Japan have stimulated the development of HSR networks in countries like Australia and India. However, the development and design of HSR networks pose unique engineering challenges. This paper explores some of these challenges and offers solutions using innovative materials and computational approaches.

One major obstacle in developing HSR networks is that the existing railway tracks are often inadequate, as they were not originally designed to accommodate high-speed trains. There are two potential solutions to address this issue: (a) strengthening the existing tracks; (b) constructing new tracks dedicated to HSR operations. Several researchers have explored techniques for strengthening the existing railway infrastructure. Farooq and Nimbalkar (2024b) developed a novel composite material composed of soil, polyurethane and scrap rubber for use in track substructure layers. This material can alleviate the settlement issues typically associated with conventional granular track substructure layers, thereby improving the track performance. Punetha and Nimbalkar (2021) examined the efficacy of utilizing geosynthetics for strengthening conventional ballasted tracks. Their findings suggest that these materials could offer cost-effective solutions for enhancing the performance of ballasted tracks for HSR operations.

Alternatively, new tracks can be constructed exclusively for HSR. However, determining the most appropriate track type presents significant challenges. Typically, ballastless (or slab) tracks are preferred for HSR networks, as seen in countries such as China, Germany and Japan, owing to their reduced thickness, lighter weight and minimal maintenance requirements. Despite these advantages, ballastless tracks are expensive to construct and absorb less noise and vibration compared to ballasted tracks (Ollivier et al., 2014). To mitigate vibration concerns associated with these tracks, the composite material developed by Farooq and Nimbalkar (2024b) could be utilized, as elaborated later in this paper.

Ballasted tracks can also be used for HSR operations, as evidenced by their use in countries like France and Spain, because of their lower initial construction cost. However, they require regular maintenance because of the cumulative plastic deformation of constituent granular layers and subgrade under repeated train-induced loads. Therefore, selection of the most adequate track type depends on various factors, including budget, design speed, axle loads, environmental impact and topography, among others. A thorough comparison of the two track types is crucial for informed decision-making, which can be effectively conducted using the finite element method (FEM), as discussed in ‘Comparative analysis of ballasted and ballastless track performance’ section.

Another significant challenge in designing HSR infrastructure is the accurate assessment of both transient and long-term behavior of railway tracks subjected to repeated loading from moving trains. This analysis is paramount for transition zones between standard track sections and stiff structures like tunnels, bridges and viaducts, which are essential for maintaining alignment and speed in HSR networks. These transitions are prone to rapid track geometry degradation due to heterogenous support conditions, which can cause uneven deformation or differential settlement (Li and Davis, 2005). To improve their performance, it is essential to have prior information of the amount of differential settlement accumulating in track layers over a specified period.

Computational approaches, such as numerical and analytical methods, can be employed to analyze the long-term performance of railway tracks. While numerical modelling accurately simulates dynamic track behavior, these models often require significant computational resources and time, particularly when predicting the cumulative plastic deformation over thousands or millions of train passages (Varandas et al., 2013). In contrast, analytical approaches, such as rheological models, offer faster and more computationally efficient alternatives for predicting long-term track performance. For example, the rheological approach proposed by Punetha and Nimbalkar (2023) predicted the behavior of a railway track at a bridge approach in 1,080 s, while the FEM took 355,615 s to solve the same problem on a high-performance computing facility with thirty 2.5 GHz processors. This demonstrates that the rheological approach is approximately 330 times more efficient than FEM. A review of rheological models suitable for predicting the track response to train-induced loading is provided in the section ‘Current state of the art on rheological models for railway tracks’. The geotechnical rheological model proposed by Punetha and Nimbalkar (2022a) for standard and transition zones is also discussed.

The final section of this paper addresses the challenges associated with the development of HSR corridors in seismically active regions. It presents a rheological model that can be utilized to assess the lateral stability of railway tracks under seismic loading, providing insights that can contribute to the earthquake-resistant design of tracks. In addition, FEM is employed to investigate the influence of seismic loading on the soil arching mechanism, which plays a critical role in the behavior of pile-supported railway embankments.

NOVEL COMPOSITE MATERIAL FOR HIGH-SPEED RAIL TRACKS

This section evaluates the performance of a novel composite material comprising soil, polyurethane and scrap rubber, in terms of damping ratio (ζ) and shear modulus (*G*). These properties were evaluated using cyclic direct simple shear (CDSS) testing to determine the optimum dosages of polyurethane and scrap rubber. Based on earlier direct simple shear tests (both static and cyclic), the optimum polyurethane content was identified as 10% (Farooq and Nimbalkar, 2024b). Using this optimal dosage, specimens with varying scrap rubber content (RC = 0–25%) were prepared and tested under different cyclic shear stress amplitude (τ_c) using the CDSS device. The results for these tests are presented below, and further details on the methodology are available in Farooq and Nimbalkar (2024b).

Fig. 1(a) illustrates the variation of *G* for soil treated with polyurethane (10%) and mixed with varying RC. It is apparent that *G* exhibits an inconsistent trend at $\tau_c = 50$ kPa, increasing from 5.76 GPa at 0% RC to 7.5 GPa at 15% RC, and subsequently decreasing to 6.49 GPa at 25% RC. At $\tau_c = 100$ kPa, *G* initially increases with a rise in RC from 0% to 2.5%, but then decreases with further increase in RC. Similarly, at $\tau_c = 200$ kPa, *G* consistently decreases with increasing RC. The maximum *G* values at $\tau_c =$ 50, 100 and 200 kPa are 7.5 GPa (at 15% RC), 6.32 GPa (at 2.5% RC) and 6.3 GPa (at 0% RC), respectively. This significant variation in *G* makes it challenging to determine the optimal RC, thereby requiring an analysis of the damping ratio to identify the optimum dosage.

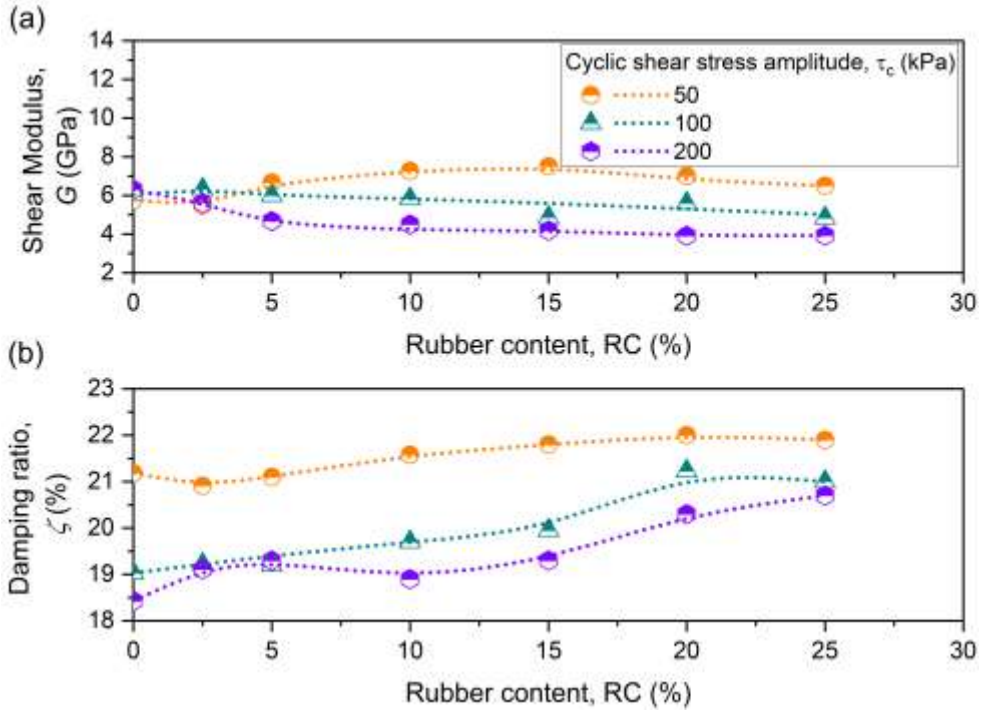

Fig. 1 Variation in (a) shear modulus and (b) damping ratio in response to cyclic shear stress amplitude and rubber content for treated soil

Fig. 1(b) depicts the variation of ζ for polyurethane-treated soil at different τ_c and RC. It is apparent that ζ decreases with an increase in τ_c, while it rises with increasing RC. The maximum ζ values at $\tau_c = 50$, 100 and 200 kPa are 22% (at 20% RC), 21.2% (at 20% RC) and 20.7% (at 25% RC), respectively. Therefore, the optimal RC for polyurethane-treated soils is considered to lie between 10–20%, achieving a desirable

ζ with minimal effects on other properties, which are discussed in detail in Farooq and Nimbalkar (2024b).

Thus, these results indicate that the incorporation of scrap rubber into polyurethane-treated soils improves the damping properties of the mix, though it is accompanied by a reduction in shear modulus at higher RC. Therefore, selecting the optimal RC is crucial and should be based on a trade-off between damping enhancement and modulus reduction. This optimization is particularly important for HSR applications, where improved damping helps mitigate vibrations, but maintaining adequate shear modulus is essential for track stability.

COMPARATIVE ANALYSIS OF BALLASTED AND BALLASTLESS TRACK PERFORMANCE

This section highlights the use of FEM to compare the performance of ballasted and ballastless tracks. Three-dimensional (3D) FE models for both track types were developed using ABAQUS (Dassault Systèmes, 2018) (see Fig. 2). In these models, the rail, sleepers, reinforced concrete slab, cement asphalt mortar (CAM) and base were modeled as elastic materials, while the ballast, subballast and subbase were simulated as elastoplastic materials following the Drucker-Prager yield condition. The subgrade was represented as a linearly elastic, perfectly plastic material following the Mohr-Coulomb yield condition. Coulomb's friction law governed the surface contact interactions between the track layers. A detailed methodology is provided in previous studies (e.g., Farooq et al., 2021, 2022). The input parameters used in the analyses for ballasted and ballastless tracks are listed in Table 1.

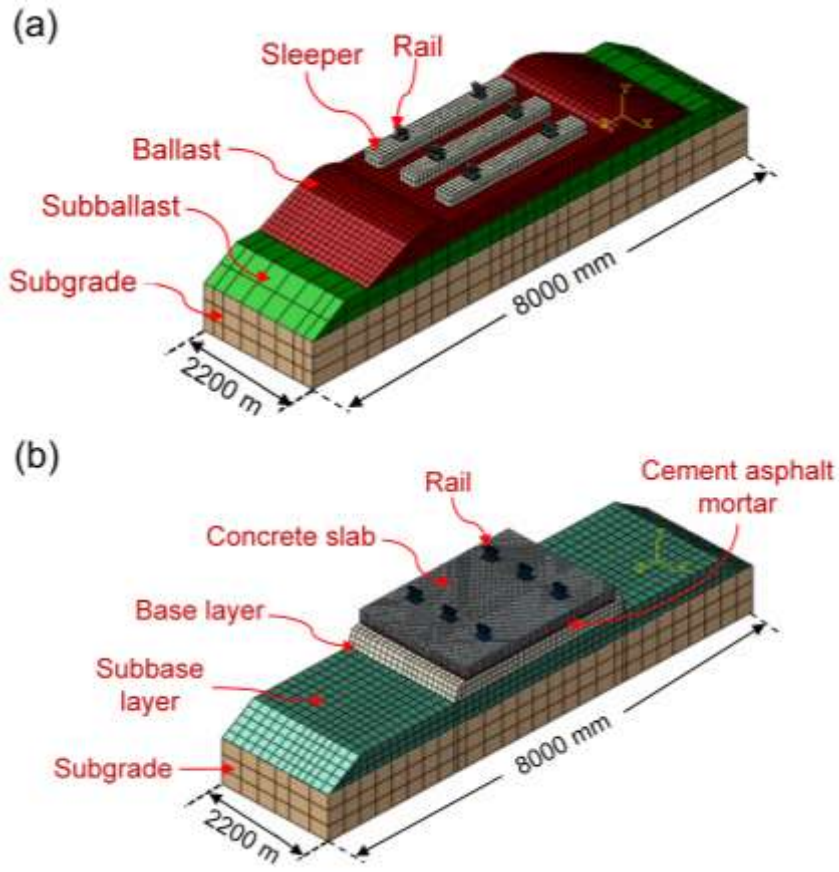

Fig. 2 3D finite element model of (a) ballasted and (b) ballastless track [modified after Farooq et al. (2021)]

Fig. 3(a) shows the distribution of vertical elastic displacement (δ_v^e) and vertical stress (σ_v) with depth in both ballasted and ballastless tracks. The data points in Fig. 3(a), labeled *BT* and *BL* followed by a number that increases with depth, represent the interfaces between the different track components for ballasted and ballastless tracks, respectively. It is apparent that the peak σ_v on the surface of both tracks, caused by the 12-ton train axle load is 5.4 MPa. The axle load of 12 tons corresponds to that exerted by a

Japanese Class–300 high-speed passenger train. In the ballasted track, σ_v decreases non-uniformly with depth, with a 74% reduction from BT1 to BT2 and a 98% reduction from BT1 to BT3. Below the ballast layer, the stress reduction is minimal. In contrast, in the ballastless track, σ_v decreases by 93.3% from BL1 to BL2 and by 96.2% from BL1 to BL3, showing significant stress dissipation within 200 mm from the top of the reinforced concrete slab. In the ballasted track, a similar stress state is observed at a depth of 550 mm from the top of the sleeper. This difference is ascribed to the higher stiffness of reinforced concrete slab, which causes wider stress distribution. In addition, σ_v at the bottom of the subgrade is 50 kPa for the ballastless track, which is half of that in the case of ballasted track.

Table 1: Input parameters used for evaluating the response of ballasted and ballastless tracks

Layer	Density, ρ (kg/m^3)	Elastic modulus, E (MPa)	Poisson's ratio, ν	Friction angle, φ (°)	Dilation angle, ψ (°)
Ballasted Track					
Rail	7830	210,000	0.30	–	–
Sleeper	2400	30,000	0.15	–	–
Ballast	1600	110	0.30	40	5
Subballast	2220	210	0.25	35	2
Subgrade	2220	400	0.25	35	2
Ballastless Track					
Rail	7830	210,000	0.30	–	–
Concrete slab	2700	20,000	0.17	–	–
Cement asphalt mortar	2250	27,000	0.17	–	–
Base layer	2700	7500	0.17	–	–
Subbase layer	2220	400	0.25	35	2
Subgrade	2220	400	0.25	35	2

Note: The damping ratio has been adopted as 0.04 for subbase, ballast, subballast and subgrade layers. Further details about the adopted parameters are provided in Farooq et al. (2021).

Fig. 3(a) also highlights that δ_v^e at BT1 in the ballasted track is 1.07 mm, decreasing by 46.7% at BT2 and 98.9% at BT3. In contrast, δ_v^e in the ballastless track is 0.058 mm at BL1, reducing by 13.8% at BL2 and 51.7% at BL3. This shows that δ_v^e at the top of the ballastless track is 95% lower than that at the top of the ballasted track. Fig. 3(b) depicts the cumulative settlement variation with number of load cycles (N) for both track types. After N = 1.2 million, the ballastless track shows a settlement of 0.295 mm, which is approximately 26 times lower than the settlement in ballasted track. These results demonstrate that ballastless tracks outperform ballasted tracks under same loading conditions. However, the selection of the most appropriate track type should also account for factors such as cost and environmental impact.

The above analysis demonstrates that ballastless tracks significantly outperform ballasted tracks in terms of stress distribution and δ_v^e, making them a superior choice for HSR applications. The reinforced concrete slab in ballastless tracks facilitates more efficient stress distribution and minimizes settlement, which is crucial for maintaining track stability and ensuring passenger comfort at high speeds. With a settlement reduction of 95% compared to ballasted tracks, ballastless systems also demonstrate long-term durability, leading to minimal maintenance requirements. However, despite these mechanical advantages, factors such as construction cost and environmental impact must be carefully evaluated when selecting the most appropriate track type.

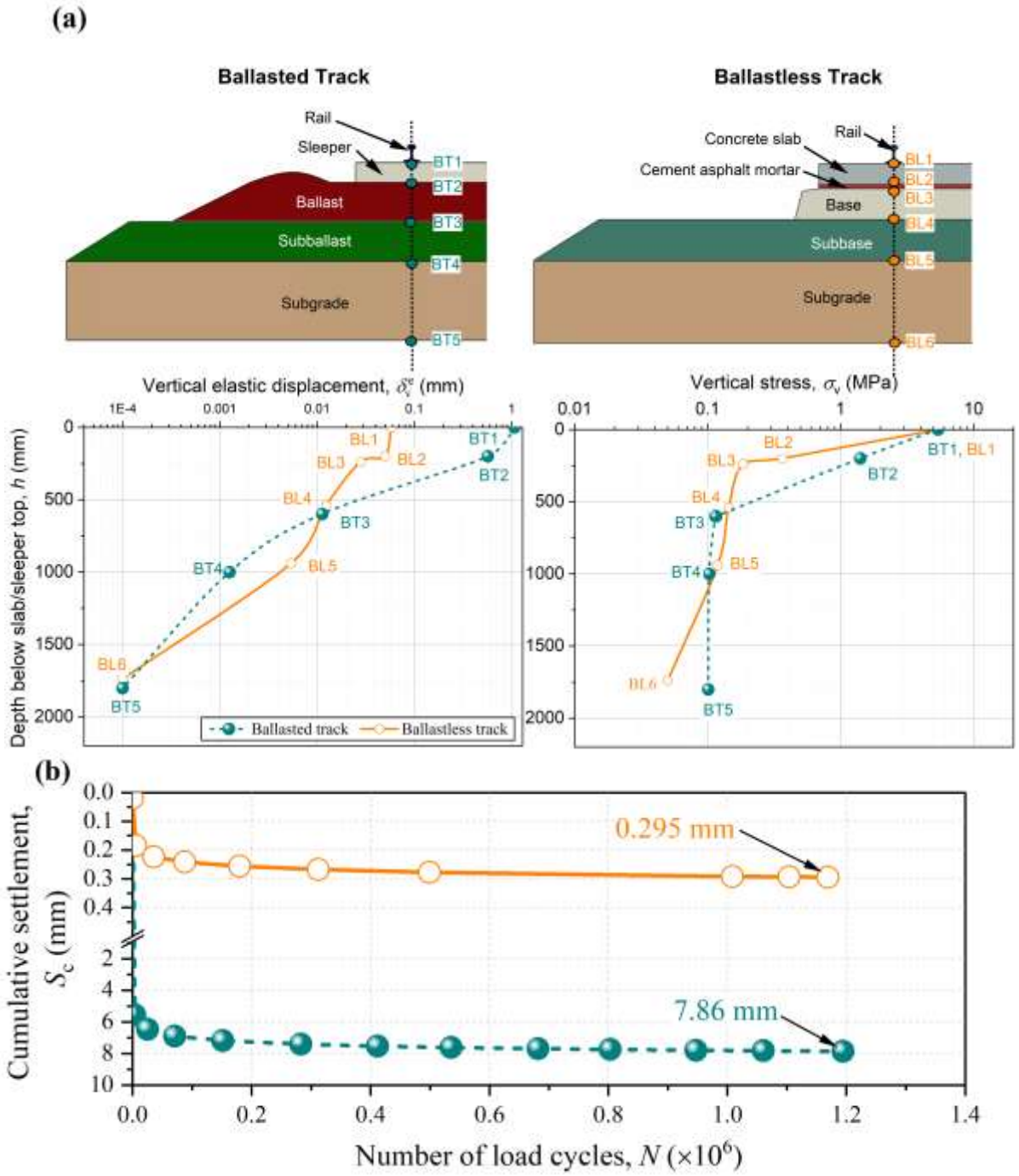

Fig. 3 (a) Attenuation of vertical elastic displacement and vertical stress with depth; (b) variation of cumulative settlement of track with number of load cycles [data taken from Farooq et al. (2021)]

CURRENT STATE OF THE ART ON RHEOLOGICAL MODELS FOR RAILWAY TRACKS

As discussed in the introduction section, the analytical approaches, such as rheological models, provide a comparatively quicker and more computationally efficient option to numerical methods for accurate evaluation of dynamic track response, especially when dealing with thousands or millions of train passages. The rheological models can capture the complex behavior of geomaterials under repeated loading, particularly the recoverable (elastic) and irrecoverable (plastic) deformations. These models simulate complex soil behavior by combining simple elements, typically representing elasticity (Hooke's element), viscosity (Newton's element) and plasticity (St. Venant's element), in various configurations (Farooq and Nimbalkar, 2024a). These configurations include viscoelastic (viscosity and elasticity), elastoplastic (elasticity and plasticity), viscoplastic (time-dependent plastic behavior), elastoviscoplastic

(elasticity, viscosity and plasticity) and viscoelastoplastic (viscoelastic behavior transitioning to plastic behavior) models (see Fig. 4).

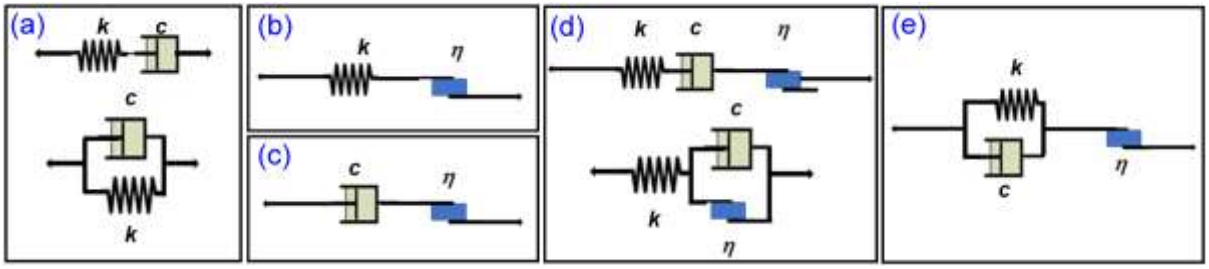

Fig. 4 Configuration of rheological models using Hooke's, Newton's and St. Venant's elements (a) viscoelastic; (b) elastoplastic; (c) viscoplastic; (d) elastoviscoplastic; (e) viscoelastoplastic

Widely used rheological models such as the Maxwell, Kelvin-Voigt, Burgers, Zener and Bingham models play a critical role in understanding the behavior of multi-layered systems like railway tracks. These models are typically used to evaluate the long-term behavior, such as settlement accumulation (Punetha et al., 2020, 2021) and creep (Liingaard et al., 2004) in tracks subjected to heavy loads and high-speed trains. In particular, viscoelastoplastic models are effective in simulating the transition from elastic to plastic behavior in geomaterials under repeated loading, providing critical insights into track stability and maintenance requirements (Punetha et al., 2021).

Previous research on track dynamics using analytical models has primarily focused on evaluating transient vertical, longitudinal and lateral responses. Earlier studies used simple models to investigate wheel-rail interactions (Lyon, 1972; Jenkins et al., 1974; Newton and Clark, 1979). Later, more complex models were introduced to study the track stability (Knothe et al., 1995) and vibrations (Zhai et al., 2004). Recently, Punetha et al. (2020, 2021) developed track models which focused on evaluating both short and long-term behavior of railway tracks subjected to repeated train loadings. These models effectively captured the elastic and plastic behavior of the geomaterials in the track substructure layers and predicted the track settlement accumulated over millions of load cycles.

Incorporating the concept of continuity in track layers (Zhai et al., 2004) and overlapped stress areas (Ahlbeck et al., 1978), the viscoelastic model developed by Punetha et al. (2020) featured a three-layered structure comprising rheological elements (springs and dashpots) having varying properties for each layer. The plastic deformation of the track substructure layers was captured through empirical equations. Subsequently, Punetha et al. (2021) proposed using plastic slider elements to simulate plastic deformation of the track substructure layers subjected to train-induced repeated loading. This model was able to predict settlement under repeated train passages and capture the influence of axle load, train speed and substructure layer thickness.

The model was subsequently extended to incorporate the inhomogeneous support conditions typically encountered in the transition zones (Punetha and Nimbalkar, 2023), influence of principal stress rotation (PSR) (Punetha and Nimbalkar, 2022a) and influence of geosynthetic reinforcement (Punetha and Nimbalkar, 2022b) on track response. Subsequently, Farooq et al. (2024) introduced a viscoelastic rheological model to evaluate the lateral stability of railway tracks, highlighting the significance of considering lateral forces in the analysis to gain a clearer insight into dynamic track behavior. The next section discusses the rheological model that incorporates the PSR effect.

GEOTECHNICAL RHEOLOGICAL MODEL FOR EVALUATING THE BEHAVIOR OF RAILWAY TRACKS UNDER MOVING LOADS

A soil element within the track substructure undergoes intricate changes in vertical, lateral and shear stresses due to moving loads, resulting in PSR (Powrie et al., 2007). Earlier laboratory studies have demonstrated that PSR has considerable impact on the accumulation of plastic deformation in track materials (Gräbe and Clayton, 2009; Ishikawa et al., 2011). The extra deformation from PSR accelerates the degradation of track geometry and stability. Therefore, it is crucial to account for PSR effects to accurately evaluate the track behavior under moving loads induced by high-speed trains.

As highlighted in the previous section, several analytical methods have been formulated to evaluate the behavior of railway tracks under repeated train passages. However, models that consider PSR effects on track behavior are rather limited. Despite their practical utility, existing computational approaches often overlook the effect of PSR, potentially reducing the accuracy of predicted track behavior.

Punetha et al. (2021) developed a computational approach based on geotechnical rheological track model to analyze both short-term and long-term behavior of railway tracks under repeated loading from moving trains. This method was later extended to incorporate the PSR effects on track response (Punetha and Nimbalkar, 2022a). In this approach, slider elements are used to simulate the plastic behavior of the geomaterials, while springs and dampers represent the viscoelastic response. The railway track is modelled as an assemblage of discrete masses connected by elastic springs, viscous dampers and plastic sliders (see Fig. 5).

To evaluate the response of track substructure to repetitive train loading, the following dynamic equilibrium equation (Equation 1) is used (Punetha and Nimbalkar, 2022a):

$$\boldsymbol{M}d\ddot{\boldsymbol{v}}_{\mathbf{i}} + \boldsymbol{C}d\dot{\boldsymbol{v}}_{\mathbf{i}} + \boldsymbol{K}d\boldsymbol{v}_{\mathbf{i}} - \boldsymbol{C}^{\mathbf{p}}d\dot{\boldsymbol{v}}_{\mathbf{i}}^{\mathbf{p}} - \boldsymbol{K}^{\mathbf{p}}d\boldsymbol{v}_{\mathbf{i}}^{\mathbf{p}} - \boldsymbol{C}^{*}\{d\dot{\boldsymbol{v}}_{\mathbf{i-1}} + d\dot{\boldsymbol{v}}_{\mathbf{i+1}}\} - \boldsymbol{K}^{*}\{d\boldsymbol{v}_{\mathbf{i-1}} + d\boldsymbol{v}_{\mathbf{i+1}}\} + \boldsymbol{C}^{\mathbf{p}^{*}}\{d\dot{\boldsymbol{v}}_{\mathbf{i-1}}^{\mathbf{p}} + d\dot{\boldsymbol{v}}_{\mathbf{i+1}}^{\mathbf{p}}\} + \boldsymbol{K}^{\mathbf{p}^{*}}\{d\boldsymbol{v}_{\mathbf{i-1}}^{\mathbf{p}} + d\boldsymbol{v}_{\mathbf{i+1}}^{\mathbf{p}}\} = d\boldsymbol{F} \quad (1)$$

where $d\boldsymbol{v}$, $d\dot{\boldsymbol{v}}$ and $d\ddot{\boldsymbol{v}}$ represent the vertical displacement, velocity, and acceleration increment vectors, respectively; $d\boldsymbol{F}$ is the force increment vector; $\boldsymbol{K}$ is the stiffness matrix; $\boldsymbol{M}$ represents the mass matrix; $\boldsymbol{C}$ denotes the damping coefficient matrix. The subscript i refers to the i^{th} sleeper, and the superscript p denotes the inelastic (or plastic) component. The PSR effect is incorporated in the constitutive equations for the sliders (Punetha and Nimbalkar, 2022a).

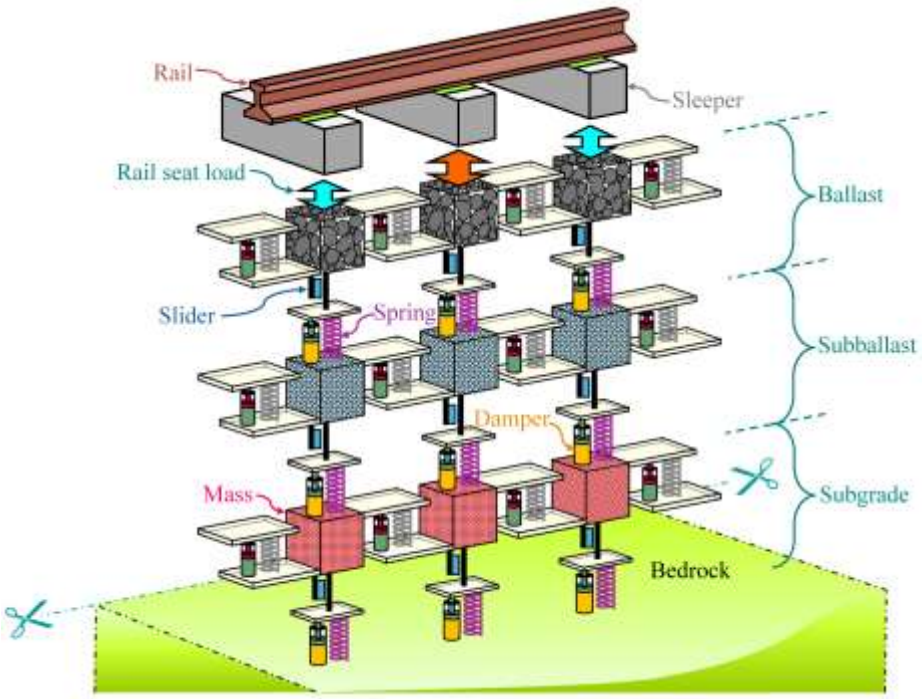

Fig. 5 Three-dimensional geotechnical rheological ballasted railway track model

Fig. 6 illustrates an example of the ballasted track response predicted using the rheological model for a standard track, accounting for PSR effects. The input parameters used in the analyses are listed in Table 2. It is apparent that track settlement is significantly greater when PSR effect is incorporated in the analysis compared to when it is ignored. At traffic tonnage of 20 million gross metric tons (MGT), the cumulative track settlement is 24.6% greater when PSR is included than when overlooked. This highlights the importance of incorporating PSR effects in the analysis to accurately evaluate track behavior. In addition, the results indicate that PSR accelerates the deterioration of track geometry. Without PSR, 15 mm cumulative settlement occurs after 3.5 MGT; however, with PSR, same magnitude of settlement is reached only after 0.43 MGT. These findings underscore the critical need to account for PSR effects in the analysis to ensure accurate assessment of track performance under repetitive moving loads.

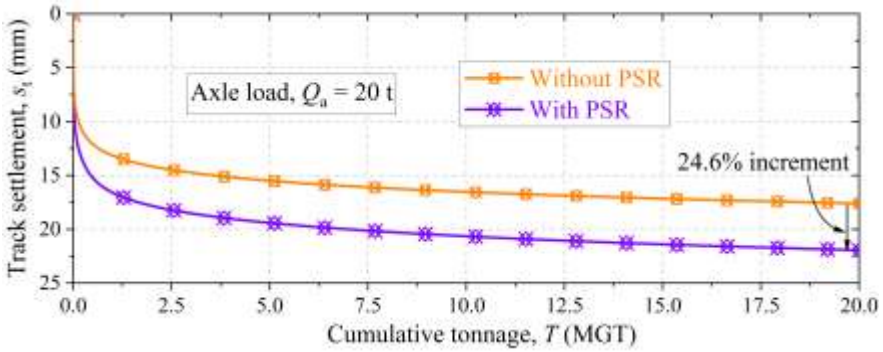

Fig. 6 Influence of principle stress rotation on cumulative track settlement [data sourced from Punetha and Nimbalkar (2022a)]

Table 2: Input parameters used for evaluating the track response [data taken from Punetha and Nimbalkar (2022a)]

Layer	Thickness, h (mm)	Density, ρ (kg/m^3)	Elastic modulus, E (MPa)	Poisson's ratio, ν	Shear stiffness, k^s (MN/m)
Ballast	300	1760	200	0.3	78.4
Subballast	150	1920	115	0.4	476
Subgrade	5000	1920	41	0.35	1600

Note: The parameters for the slider elements for ballast, subballast and subgrade are provided in Punetha and Nimbalkar (2022a)

Application to Transition Zones

The computational approach discussed in the previous section can also be applied to analyze the behavior of tracks along the transition zones, where support conditions vary along the length of the track (Punetha and Nimbalkar, 2023). Fig. 7 depicts the response of a ballasted railway track in a bridge approach, predicted using the rheological approach with and without considering PSR effects. In this example, the stiffer side of track substructure comprises a ballast layer overlying the bridge deck, while the softer side consists of ballast and subballast layers overlying the subgrade (Punetha and Nimbalkar, 2022a). The bridge deck and abutment are modeled as fixed supports because they undergo significantly less deformation than the geotechnical track layers.

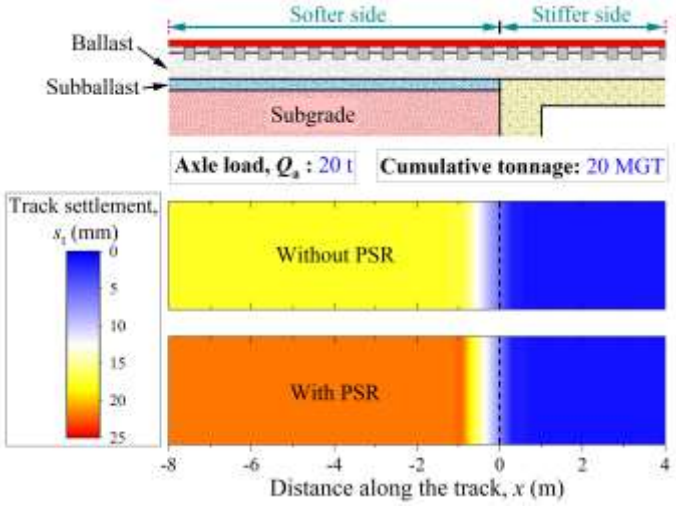

Fig. 7 Settlement variation along the track with and without considering the PSR effect [data sourced from Punetha and Nimbalkar (2022a)]

As illustrated in Fig. 7, the differential settlement in a standard track-bridge transition zone is significantly greater when PSR is considered, compared to when it is neglected. In other words, neglecting PSR effects leads to a substantial underestimation of differential settlement in transition zones. These findings highlight the importance of incorporating PSR effects in computational models to accurately predict railway track behavior under high-speed moving loads.

SEISMIC LATERAL STABILITY OF RAILWAY TRACKS

The railway tracks for HSR operations in seismically active regions must withstand lateral dynamic forces induced by earthquakes, which can cause significant deformations in geotechnical layers, rail buckling, damage to fasteners and potential track failure. Therefore, it is crucial to assess the stability of railway tracks under lateral loading. Several computational models have been developed to evaluate the stability of railway tracks under lateral loads (Hoseini et al., 2019; Nakamura et al., 2011; Esmaeili and Noghabi, 2013). However, these models are simplistic and mainly focus on vertical responses, overlooking critical lateral deformations.

Farooq et al. (2024) developed a viscoelastic rheological model to simulate track behavior under lateral dynamic loads. This model accurately captures both vertical and lateral track displacements, allowing precise prediction of track stability and identification of scenarios where lateral forces may exceed safety limits. It also provides a framework to gain insights into the influence of different track parameters on the lateral response, which is crucial for assessing seismic stability. Fig. 8 illustrates an example of the track response evaluated using the rheological model under different ballast and subballast thickness. The input parameters used in the analysis are listed in Table 3. It is apparent that the lateral displacement at the ballast top decreases with a rise in ballast and subballast thickness, suggesting that thicker granular layers would outperform thinner layers during seismic events. Thus, this approach can be utilized to assess the risk of track failure during earthquakes and the effectiveness of mitigation strategies aimed to enhance the lateral track stability.

Table 3: Input parameters for evaluating the lateral track response [data taken from Farooq et al. (2024)]

Layer	Thickness, h (m)	Density, ρ (kg/m^3)	Elastic modulus, E (MPa)	Poisson's ratio, ν	Shear stiffness, k^s (MN/m)
Ballast	0.35−0.75	1900	250	0.4	1
Subballast	0.25−0.50	1920	120	0.4	476
Subgrade	3	1920	20	0.4	1600

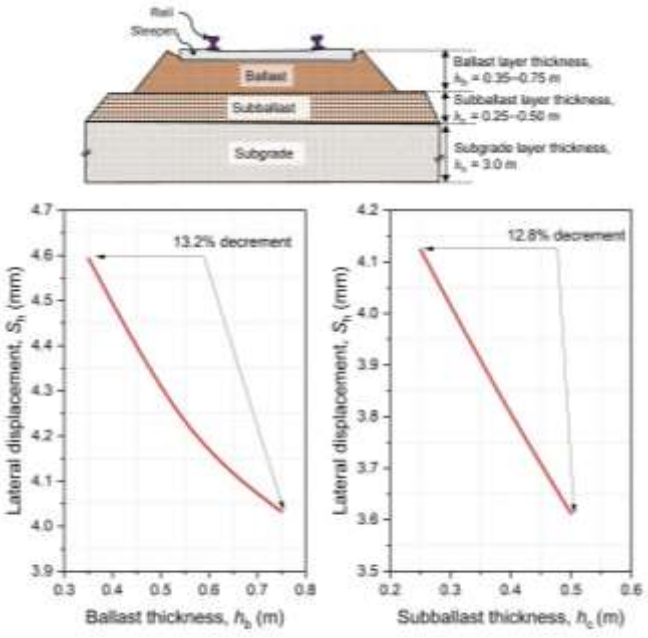

Fig. 8 Influence of ballast and subballast thickness on track lateral stability

SEISMIC ASSESSMENT OF SOIL ARCHING MECHANISM IN A GEOSYNTHETIC-REINFORCED PILE FOUNDATION SUPPORTED EMBANKMENT

Often, HSR corridors are required to be constructed on challenging ground conditions (e.g., soft soils) and even in seismically active regions (Deng et al., 2024). Several ground improvement techniques are available to enhance the ground conditions and provide a stable base for these corridors. Among all ground improvement techniques, geosynthetic-reinforced pile-supported (GRPS) embankments provide a highly effective solution, enhancing construction speed while reducing differential settlement. In these embankments, most of the load from the embankment fill and moving trains is transmitted to pile foundations via a mechanism referred to as soil arching. Additionally, geosynthetic layers improve the load transfer to pile foundations by means of the tensioned membrane effect.

To date, the mechanism of soil arching in GRPS embankments has been thoroughly studied under both static and traffic-induced cyclic loading (Niu et al., 2018; Pham and Dias, 2021). Niu et al. (2018) carried out model tests on an instrumented GRPS embankment. A servo-hydraulic actuator was considered to replicate load induced by a moving train. It was found that soil arching zone reduced under the high-speed train-induced load in comparison to the static load condition. Furthermore, accumulated settlement and geogrid strain exhibited an almost constant and increasing trend, respectively, after long-term loading. Pham and Dias (2021) carried out 3D numerical analyses to evaluate the influence of GRPS embankment parameters on soil arching. The study concluded that the properties of the embankment fill, stiffness of subsoil and the ratio of embankment height (h_{em}) to pile spacing (s) are the most influential factors to consider in design methods. However, the mechanism of soil arching in pile foundation supported embankments under earthquake-induced loading is not completely understood.

In view of this, Meena and Nimbalkar (2021) numerically simulated a GRPS embankment in two-dimensional (2D) plane-strain condition to assess the mechanism of soil arching under earthquake-induced loading. The numerical model was developed using ABAQUS (Dassault Systèmes, 2018) and converted from a 3D model to 2D using appropriate conversion method (Meena et al., 2020; Meena et al., 2021). In addition to the self-weight of the track layers, an equivalent dynamic load generated by the moving trains was applied to the top of the fill.

Fig. 9 illustrates a schematic diagram of a typical GRPS embankment, including the analyzed region. The simulated model comprises a hard stratum underlying 8 m thick subsoil and end-bearing pile foundations. The parameters s and h_{em} are set at 2.5 m and 3.5 m (including a 0.4 m thick gravel cushion at the base), respectively. Additionally, a geosynthetic layer (2 mm thick) is placed in the middle of the gravel cushion. The input parameters used in the numerical analysis to investigate soil arching in a GRPS embankment are listed in Table 4. The slope of the GRPS embankment is disregarded during numerical analysis to prevent its influence on soil arching.

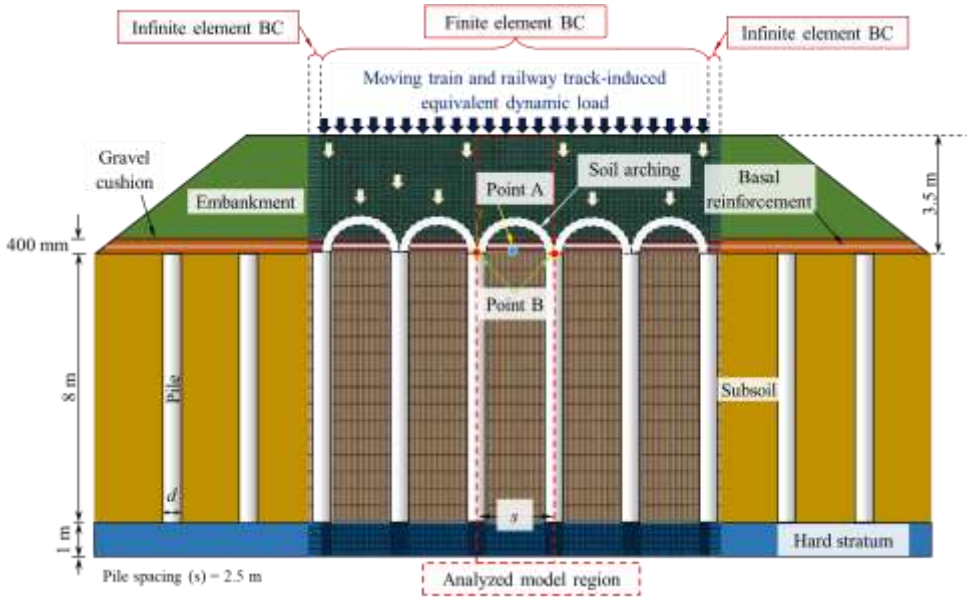

Fig. 9 Schematic diagram of a typical GRPS embankment, including the analyzed region

Table 4: Input parameters used to investigate soil arching in the GRPS embankment [data taken from Meena and Nimbalkar (2021)]

Material properties	Embankment fill	Gravel bed	Subsoil	Geosynthetic layer (at 2% tensile strain)
Constitutive model	MC	MC	MCC	LE
Unit weight, γ (kN/m^3)	20	21	18.4	–
Young's modulus, E (MPa)	20	25	–	500
Poisson's ratio, v	0.25	0.25	0.30	0.30
Effective cohesion, c' (kPa)	0.1	0.1	–	–
Effective friction angle, φ' (°)	30	35	–	–
Effective dilation angle, ψ' (°)	0	5	–	–
Critical stress ratio, M	–	–	1.2	–
Logarithmic hardening constant, λ	–	–	0.06	–
Logarithmic bulk modulus, k	–	–	0.012	–
Initial yield surface size, a_o (kPa)	–	–	103	–
Void ratio at unit pressure, e_1	–	–	0.87	–
Initial void ratio, e_o	–	–	0.45	–
Geosynthetic stiffness, J (kN/m) = $E \times t$	–	–	–	1000

Note: LE: Linear elastic; MC: Mohr-Coulomb; MCC: Modified Cam-Clay

Further details on model validation and methodology are reported elsewhere (see Meena et al., 2020; Meena et al., 2021; Nimbalkar and Meena, 2022).

Fig. 10 illustrates the vertical stress distribution trend above point A (refer to Fig. 9) within the embankment fill for three scenarios: (i) unreinforced (i.e., without geosynthetic reinforcement) + no earthquake (EQ); (ii) unreinforced + EQ; (iii) reinforced + EQ. The unreinforced + no EQ scenario is considered as the nominal case to allow better comparison of different scenarios.

For the nominal case, it can be observed that the vertical stress aligns with the geostatic stress profile from the top of the embankment down to a height (h_{em}) of 2.3 m, which marks the outer edge of soil arch. Subsequently, the vertical stress decreases up to 0.6 m height, which indicates the inner edge of soil arch. A slight increase in vertical stress is observed below the inner edge of the soil arch, attributed to the self-weight of the soil. The primary cause of the reduction in vertical stress is the transfer of majority of stress to the pile heads instead of subsoil, due to soil arching. The area between the outer and inner edges of the soil arch is referred to as the soil arching zone.

Conversely, for the unreinforced + EQ case, the vertical stress increases linearly from the top to the base of the embankment, suggesting that soil arching is not mobilized under seismic loading. Furthermore, the reinforced + EQ case demonstrates that the reinforcement aids in the mobilization of soil arching during seismic conditions. The vertical stress first rises from the top of the embankment to h_{em} = 1.9 m, indicating the outer edge of soil arch. However, the trend does not follow geostatic stress profile due to the horizontal excitation caused by the earthquake. Beyond this point, the stress decreases down to 0.5 m, representing the inner edge of soil arch. Additionally, the vertical stress at the embankment base is much less in comparison to the unreinforced case. Thus, Fig. 10 indicates that geosynthetic reinforcement improves soil arching mobilization in pile foundation supported embankments under seismic conditions.

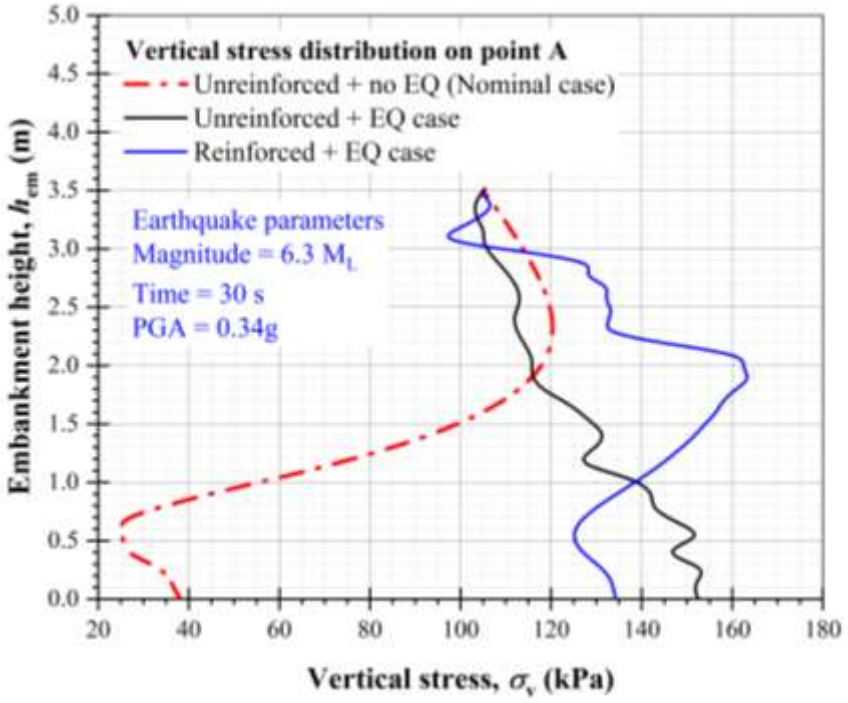

Fig. 10 Vertical stress distribution trend above point A within the embankment fill for different scenarios [data sourced from Meena and Nimbalkar (2021)]

Fig. 11 depicts the soil arching ratio (*SAR*) at point A in the GRPS embankment for both static and seismic conditions. *SAR* is defined as the ratio of vertical stress on the subsoil to the total overburden stress, which includes the surcharge (see Equation 2).

$$SAR = \frac{\sigma_{\text{subsoil}}}{[(\gamma.h_{\text{em}})+q]} \tag{2}$$

where, σ_{subsoil} refers to the vertical stress within the embankment fill along the point A; γ denotes the unit weight of embankment fill, q refers to the equivalent dynamic load. *SAR* ranges from 0 to 1, where a value of 0 indicates that the entire embankment load, including the surcharge, is transmitted to the pile heads (i.e., complete mobilization of soil arching). A value of 1 indicates the absence of soil arching, meaning the vertical stress on the subsoil is equal to the total overburden stress, which includes the surcharge.

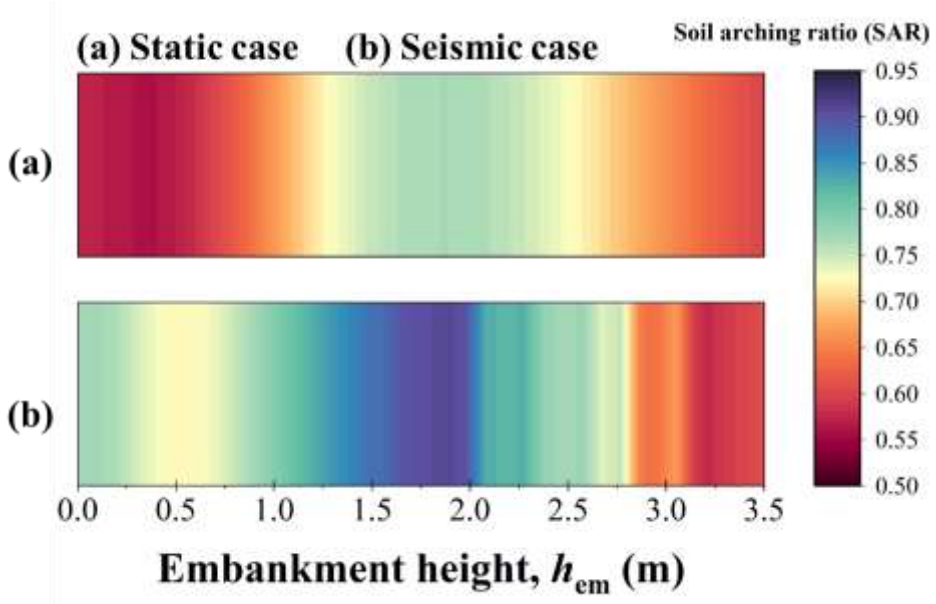

Fig. 11 Influence of earthquake loading on soil arching ratio at point A in the GRPS embankment for (a) static case; (b) seismic case [data sourced from Meena and Nimbalkar (2021)]

It is evident from Fig. 11 that SAR at embankment base is 0.57 for static condition and 0.77 for seismic condition. It decreases up to h_{em} = 0.3 m for static condition and 0.5 m for earthquake condition. This embankment height delimits the inner edge of the soil arch. Subsequently, SAR in both conditions increases with a rise in h_{em} up to 1.9 m. This height corresponds to the outer edge of the soil arch.

Thus, these findings indicate that soil arching is significantly impacted by earthquake loading. The incorporation of geosynthetic reinforcement has the potential to mobilize soil arching more effectively and efficiently, even during a seismic event. Consequently, the implementation of geosynthetic layers is recommended for railway embankments that are supported by pile foundations, regardless of their location in either seismically active or inactive regions.

CONCLUDING REMARKS

This keynote paper explored key engineering challenges associated with the design and development of HSR networks. Key issues identified include the need to reinforce or replace existing tracks, the prediction of long-term track performance, the management of transition zones and the improvement of seismic resilience. To address these issues effectively, the applications of innovative composite materials, along with analytical and numerical techniques, have been demonstrated. Laboratory investigations revealed that a novel composite material comprising soil, scrap rubber and polyurethane can significantly improve damping properties and help mitigate vibration problems in ballastless tracks. Numerical method, particularly FEM, has proven highly effective in comparing the performance of ballasted and ballastless tracks, providing critical insights for informed decision making on the most appropriate track type for HSR operations. Nevertheless, predicting the long-term behavior of railway tracks under repeated loading remains a challenge for FEM due to extensive computational time required. Alternatively, analytical methods based on rheological models offer a more efficient means to assess the long-term behavior of HSR tracks. These models proved effective in predicting the performance of tracks in both standard sections and transition zones, providing crucial information for optimizing the design. These models can also be employed to evaluate the lateral stability of railway tracks in seismically active regions, aiding in assessing the effectiveness of mitigation strategies aimed at enhancing lateral track stability. Finally, the findings from FEM revealed that soil arching in railway embankments supported by pile foundations is significantly affected by earthquake excitation. However, the incorporation of geosynthetic reinforcement can improve soil arching mechanism during seismic events, thereby improving the stability of pile-supported embankments. Thus, this paper demonstrated the effectiveness of innovative materials and computational techniques in addressing the challenges associated with the development of HSR infrastructure. As global interest in HSR continues to grow, these approaches can play a critical role in improving the safety, reliability and cost-effectiveness of HSR networks.

REFERENCES

1. Ahlbeck, D.R., Meacham, H.C. and Prause, R.H. (1978). “The development of analytical models for railroad track dynamics”, *In: Kerr, AD (ed.) Railroad Track Mechanics and Technology. London: Pergamon*.
2. Australian Federal Government (2024). “2024-25 Federal Budget”, https://www.infrastructure.gov.au/ *[Accessed 21/09/2024]*.
3. Dassault Systèmes (2018). “Abaqus (Version 2018)”, *Dassault Systèmes Simulia Corp, Providence, United States*.
4. Deng, W., Wang, C., Ou, Q., Ding, X., Luan, L., Xu, Y. and Feng, H. (2024). “Seismic response of pile-supported embankment in unequal thickness liquefiable soil with V shape underlying stratum”, *Soil Dyn Earthq Eng*, Vol. 182, pp. 108757. https://doi.org/10.1016/j.soildyn.2024.108757
5. Esmaeili, M. and Noghabi, H.H. (2013). “Investigating Seismic Behavior of Ballasted Railway Track in Earthquake Excitation Using Finite-Element Model in Three-Dimensional Space”, *J Transp Eng*, Vol. 139, No. 7, pp. 697-708. https://doi.org/10.1061/(asce)te.1943-5436.0000535
6. Farooq, H. and Nimbalkar, S. (2024a). “Rheological modelling for train-track-ground: a review from core concepts to materials and applications”, *App Eng Sci*, Vol. 20, pp. 100194. https://doi.org/10.1016/j.apples.2024.100194
7. Farooq, H., Nimbalkar, S., Punetha, P. and Sheng, D. (2024). “Viscoelastic Rheological Modelling of the Lateral Dynamic Response of Ballasted Railway Tracks”, *Transp Infrastruct Geotechnol*, Vol. 11, pp. 3667-93. https://doi.org/10.1007/s40515-024-00428-0

8. Farooq, M.A. and Nimbalkar, S. (2024b). "Static and cyclic performance of polyurethane foam adhesive bound soil–rubber mixtures under drained conditions", *Acta Geotech*, Vol. 19, pp. 561–589. https://doi.org/10.1007/s11440-023-01896-3
9. Farooq, M.A., Nimbalkar, S. and Fatahi, B. (2021). "Three-dimensional finite element analyses of tyre derived aggregates in ballasted and ballastless tracks", *Comput. Geotech.*, Vol. 136, pp. 104220. https://doi.org/10.1016/j.compgeo.2021.104220
10. Farooq, M.A., Nimbalkar, S. and Fatahi, B. (2022). "Sustainable Applications of Tyre-Derived Aggregates for Railway Transportation Infrastructure", *Sustainability*, Vol. 14, No. 18, pp. 11715. https://doi.org/10.3390/su141811715
11. Gräbe, P.J. and Clayton, C.R.I. (2009). "Effects of principal stress rotation on permanent deformation in rail track foundations", *J Geotech Geoenviron Eng*, Vol. 135, No. 4, pp. 555-565. https://doi.org/10.1061/(ASCE)1090-0241(2009)135:4(555)
12. Hoseini, S.S., Ghanbari, A. and Davoodi, M. (2019). "A New Approach in Equivalent Spring-Dashpot Method for Seismic Soil-Structure Interaction Analysis of Long Bridges Including Non-uniform Excitations", *Transp Infrastruct Geotechnol*, Vol. 6, No. 3, pp. 165-188. https://doi.org/10.1007/s40515-019-00076-9
13. Ishikawa, T., Sekine, E. and Miura, S. (2011). "Cyclic deformation of granular material subjected to moving-wheel loads", *Can Geotech J*, Vol. 48, No. 5, pp. 691-703. https://doi.org/10.1139/t10-099
14. Jenkins, H., Stephenson, J., Clayton, G., Morland, G. and Lyon, D. (1974). "The effect of track and vehicle parameters on wheel/rail vertical dynamic forces", *Railw Eng J*, Vol. 3, No. 1.
15. Knothe, K., Wu, Y. and Gross-Thebing, A. (1995). "Simple, Semi-Analytical Models for Discrete-Continuous Railway Track and their Use for Time-Domain Solutions", *Veh Syst Dyn*, Vol. 24(sup1), pp. 340-352. https://doi.org/10.1080/00423119508969635
16. Li, D. and Davis, D. (2005). "Transition of railroad bridge approaches", *J Geotech Geoenviron Eng*, Vol. 131, No. 11, pp. 1392-1398. https://doi.org/10.1061/(ASCE)1090-0241(2005)131:11(1392)
17. Liingaard, M., Augustesen, A. and Lade, P.V. (2004). "Characterization of Models for Time-Dependent Behavior of Soils", *Int J Geomech*, Vol. 4, No. 3, pp. 157-177. https://doi.org/10.1061/(ASCE)1532-3641(2004)4:3(157)
18. Lyon, D. (1972). "The calculation of track forces due to dipped rail joints, wheel flats and rail welds", *In: Second ORE colloquium on technical computer programs, Derby, UK.*
19. Meena, N.K. and Nimbalkar, S. (2021). "Soil Arching in Geosynthetic-Reinforced Pile-supported Railway Embankments under the Seismic Condition", *In: Australian Earthquake Engineering Society (AEES) 2021 Virtual Conference.*
20. Meena, N.K., Nimbalkar, S. and Fatahi, B. (2021). "Finite element analysis of soil arching in piled embankment", *In: Barla, M, Di Donna, A Sterpi, D (eds.) Challenges and Innovations in Geomechanics. IACMAG Springer International Publishing, Cham, Switzerland*, pp. 817-824.
21. Meena, N.K., Nimbalkar, S., Fatahi, B. and Yang, G. (2020). "Effects of soil arching on behavior of pile-supported railway embankment: 2D FEM approach", *Comput Geotech*, Vol. 123, pp. 103601. https://doi.org/10.1016/j.compgeo.2020.103601
22. Nakamura, T., Sekine, E. and Shirae, Y. (2011). "Assessment of Aseismic Performance of Ballasted Track with Large-scale Shaking Table Tests", *Quarterly Report of RTRI*, Vol. 52, No. 3, pp. 156-162. https://doi.org/10.2219/rtriqr.52.156
23. Newton, S. and Clark, R. (1979). "An investigation into the dynamic effects on the track of wheelflats on railway vehicles", *J Mech Eng Sci*, Vol. 21, No. 4, pp. 287-297.
24. Nimbalkar, S. and Meena, N.K. (2022). "Static and Seismic Assessment of Soil Arching in Piled Embankments", *In: Kolathayar, S, Pal, I, Chian, SC Mondal, A (eds.) Civil Engineering for Disaster Risk Reduction. Singapore: Springer Nature*.
25. Niu, T., Liu, H., Ding, X. and Zheng, C. (2018). "Model tests on XCC-piled embankment under dynamic train load of high-speed railways", *Earthq Eng Eng Vib*, Vol. 17, No. 3, pp. 581-594. https://doi.org/10.1007/s11803-018-0464-7
26. Ollivier, G., Sondhi, J. and Zhou, N. (2014). "High-Speed Railways in China: A Look at Construction Costs", *China Transport Topics*, No. 9, pp. 1-8.
27. Pham, T.A. and Dias, D. (2021). "3D numerical study of the performance of geosynthetic-reinforced and pile-supported embankments", *Soils Found*, Vol. 61, No. 5, pp. 1319-1342. https://doi.org/10.1016/j.sandf.2021.07.002
28. Powrie, W., Yang, L.A. and Clayton, C.R.I. (2007). "Stress changes in the ground below ballasted railway track during train passage", *Proc Inst Mech Eng F J Rail Rapid Transit*, Vol. 221, No. 2, pp. 247-262. https://doi.org/10.1243/0954409jrrt95
29. Punetha, P. and Nimbalkar, S. (2021). "Performance Improvement of Ballasted Railway Tracks for High-Speed Rail Operations", *Challenges and Innovations in Geomechanics. Cham, Switzerland: Springer International Publishing*.

30. Punetha, P. and Nimbalkar, S. (2022a). "Geotechnical rheological modeling of ballasted railway tracks considering the effect of principal stress rotation", *Can Geotech J*, Vol. 59, No. 10, pp. 1793-1818. https://doi.org/10.1139/cgj-2021-0562
31. Punetha, P. and Nimbalkar, S. (2022b). "Performance improvement of ballasted railway tracks using three-dimensional cellular geoinclusions", *Geotext Geomembr*, Vol. 50, No. 6, pp. 1061-1082. https://doi.org/10.1016/j.geotexmem.2022.06.007
32. Punetha, P. and Nimbalkar, S. (2023). "An innovative rheological approach for predicting the behaviour of critical zones in a railway track", *Acta Geotech*, Vol. 18, pp. 5457–5483. https://doi.org/10.1007/s11440-023-01888-3
33. Punetha, P., Nimbalkar, S. and Khabbaz, H. (2020). "Analytical evaluation of ballasted track substructure response under repeated train loads", *Int J Geomech*, Vol. 20, No. 7, pp. 04020093. https://doi.org/10.1061/(ASCE)GM.1943-5622.0001729
34. Punetha, P., Nimbalkar, S. and Khabbaz, H. (2021). "Simplified geotechnical rheological model for simulating viscoelasto-plastic response of ballasted railway substructure", *Int J Numer Anal Methods Geomech*, Vol. 45, No. 14, pp. 2019-2047. https://doi.org/10.1002/nag.3254
35. UIC (2018). "High speed rail: Fast track to sustainable mobility", *International Union of Railways (UIC): Paris*.
36. Varandas, J.N., Hölscher, P. and Silva, M.A.G. (2013). "Settlement of ballasted track under traffic loading: Application to transition zones", *Proc Inst Mech Eng F J Rail Rapid Transit*, Vol. 228, No. 3, pp. 242-259. https://doi.org/10.1177/0954409712471610
37. Zhai, W.M., Wang, K.Y. and Lin, J.H. (2004). "Modelling and experiment of railway ballast vibrations", *Journal of Sound and Vibration*, Vol. 270, No. 4-5, pp. 673-683. https://doi.org/10.1016/s0022-460x(03)00186-x